

## Synthesis of solid enantioselective macromer of trimesic acid for the enantiomeric separation of chiral alcohols

Pravin G. Ingole<sup>\*1,2</sup>, Hari C. Bajaj<sup>2</sup> and Kripal Singh<sup>2</sup>

<sup>1</sup>Greenhouse Gas Research Center, Korea Institute of Energy Research (KIER) 152 Gajeong-ro, Yuseong-gu, Daejeon 305-343, Korea

<sup>2</sup>Central Salt & Marine Chemicals Research Institute, Council of Scientific and Industrial Research (CSIR-CSMCR), Bhavnagar, Gujarat, India-364 002

(Received June 1, 2012, Revised November 28, 2012, Accepted January 3, 2013)

**Abstract.** Enantioselective macromer of trimesic acid was prepared using *S*(-)-menthol with trimesoyl chloride on polyimide (PI) ultrafiltration membrane. The chemical composition of macromer as well as polyimide ultrafiltration membrane was determined by ATR-FTIR Spectroscopy. The optical resolution of chiral alcohols was performed in pressure driven process. The effect of monomer solutions concentration, effect of air-drying time of *S*(-)-menthol solution, effect of reaction time, effect of operating pressure, effect of feed concentration of racemate on the performance of macromer was studied. The synthesised material exhibits separation of chiral alcohols (menthol ~23% and sobrelol ~21%).

**Keywords:** chiral alcohols; enantioselective membrane; polyimide; optical resolution

### 1. Introduction

The instant challenge facing by membrane separation technology is to achieve the high selectivity while retaining the productivity. A superior membrane must be able to maintain its separation properties in the complex and rigorous environment. Many extensive works have been carried out in tailoring the chemical structure/composition to improve the separation properties. Among these, cross-linking modification is one of the most comprehensive approaches (Baker 2002, Koros and Fleming 1993, Stern 1994, Koros and Mahajan 2000). Optical resolution is a very important separation process, in the field of medicine and agricultural chemicals because of their effectiveness and safety. Optically active compounds are closely related to biological and pharmacological activity and their development as an effective method for producing optically active compound is very important. The separation of enantiomers from racemic mixtures is an easy and convenient route to get optically pure compounds. The enantioseparation can be performed by several methods including chromatography, diastereomer formation and preferential crystallization (Jacques and Collet 1981, Nohira *et al.* 1976). Chromatographic methods particularly gas-liquid (GLC) (Asztemborska *et al.* 2003) and solid-liquid (HPLC) (Lough 1989,

---

\*Corresponding author, Senior Researcher, E-mail: [pgingole@kier.re.kr](mailto:pgingole@kier.re.kr)

Stevenson and Wilson 1990, Ahuja 1991) chromatography are best approaches for optical resolution at analytical scale. The liquid chromatography is an efficient method at preparative scale (Schurig 2001, Ramdeehul *et al.* 1998) however all chromatographic methods are batch processes (Xu *et al.* 2005). Enantioseparation through membrane process is promising because membrane processes are continuous, eco-friendly, economical and easy to scale up.

Enantioselective transport had also been realized for combinations of porous membranes with chiral selector groups, including biomolecules (Noble 1992, Ulbricht 2006). Proteins, such as BSA, immobilized in the pores of UF or MF membranes are presumably the best-studied example (Randon *et al.* 2000, Nakamura *et al.* 1999). The surface modification of a MF membrane with chiral polyglutamates had also yielded membranes with some enantioselectivity (Lee and Frank 2002). Liquid membranes containing enantiomer recognizing carriers such as chiral crown ether show highly enantioselective permeability (Newcomb *et al.* 1974) but low durability because losses of the liquid and carriers cannot be avoided. Some works on this area are reported by Keurentjes *et al.* (Keurentjes *et al.* 1996).

Research towards solid membranes is focused on two alternatives: the use of chiral or achiral polymers. Optical resolution through solid membrane is expected to be effective for a large amount of racemic compounds. Enantioselective permeation through a polymer membrane was first demonstrated using poly-L-glutamates with amphiphilic n-nonylphenoxy-oligo-ethyleneglycol side chains (Maruyama *et al.* 1990). In diffusion experiments with tryptophan and tyrosin, selectivities of >8 for the D vs. L-isomers had been observed (Ulbricht 2006). Aoki *et al.* (1995) and Teraguchi *et al.* (Shinohara *et al.* 1995, Aoki *et al.* 1995, 1996, 1997, 1999, Aoki 1999, Teraguchi and Masuda 2002, Teraguchi *et al.* 2003, 2005) reported some chiral membranes for optical resolution.

In this present study, we used macromer of trimesic acid for resolution of racemic alcohols. For this purpose we developed a new method for preparation of enantioselective materials and studied their performance in enantioselective permeation.

## 2. Materials and methods

### 2.1 Materials

Racemic menthol, S(-) menthol, R(+) menthol, (±)trans-sobrerol, trimesic acids and polyimide were from Sigma-Aldrich USA. N-Methyl-2-pyrrolidone (NMP), 1, 4-dioxane, hexane, methanol and other solvents were of analytical grade from SD fine Ltd. India.

### 2.2 Methods

#### 2.2.1 Preparation of enantioselective macromer - Preparation of polyimide membrane

The micro-porous polyimide membrane used as support membrane for composite membrane was prepared by diffusion induced phase separation (DIPS) technique (Wang *et al.* 1999, Lin *et al.* 2002). The phase inversion was achieved by immersion of membrane in coagulation bath such method is referred as wet phase inversion technique and widely used for the preparation of micro-porous membranes. A homogeneous solution of polyimide 16% (W/W) was prepared by dissolving

Table 1 Characteristics of polyimide membrane

S. No.	Characteristics	Value
1	Polymer content in casting solution	16% by weight
2	Thickness ( $\mu\text{m}$ )	40-50
3	Bubble point pressure (psi)	34.064
4	Bubble point diameter ( $\mu\text{m}$ )	0.3609
5	Diameter at maximum pore size distribution ( $\mu\text{m}$ )	0.2056

polyimide polymer in N-Methyl-2-pyrrolidone (NMP) and 1, 4-dioxane solvents (70:30 ratio) under continuous stirring at 55-60 °C to get homogeneous solution. The polymer solution was evacuated to remove air bubbles before casting on a non-woven polyester fabric 'Nordyl' (Filtration Sciences Corporation, USA; thickness 90-110 micrometer) under controlled conditions of temperature (25-26 °C) and relative humidity (30-35%). The membrane was air exposed for 30 sec before precipitation in de-ionized water (97.9%) containing DMF (2%) and sodium lauryl sulphate (SLS) (0.1%). Additives such as SLS and DMF are added in the coagulation bath to achieve proper properties of the membrane. The SLS is surfactant and provides proper wetting to the membrane and DMF being solvent of polymer provides progressive coagulation to get desired membrane morphology. The membrane was removed from the precipitation solution after 30 min and was washed thoroughly with de-ionized water to remove surfactant and solvent. The polyimide membrane prepared above was characterized before coating enantiomers selective layer on it. The characteristics of polyimide membrane given in Table 1 wherein porosity measurements (bubble point diameter, bubble point pressure and diameter at maximum pore size distribution) were determined by Capillary Flow Porometer (Porous Materials Inc., USA, Model CFP AEX 1500) using dry air and molecular weight cut off (MWCO) was determined by gel permeation chromatography (Water Inc., USA) using dextran solutes.

#### ***- Preparation of chiral macromer of trimesic acid on the surface of polyimide membrane***

The chiral macromer of trimesic acid was prepared on the surface of polyimide membrane by esterification reaction of 1-2% solution of trimesic acid in 60:40 water/MeOH, with 0.5-1% *S*(-) menthol (in hexane) at 60 °C. Thoroughly washed polyimide membrane was immersed in an water/MeOH solution of trimesic acid for 10 min followed by draining off for 10-20 min to remove excess solution and then immersed into *S*(-) menthol solution in hexane for 3-5 min. The esterification reaction occurs at the surface of polyimide membrane resulting in formation of an ultrathin layer of cross-linked co-polyester having chiral carbon atoms. The macromer so obtained was cured in hot air circulation at 60-70 °C for 10 min whereby polyester layer attains chemical stability. The reaction scheme of polyester formation in between *S*(-) menthol and trimesic acid has been shown as Fig. 1.

#### ***2.2.2 Characterization of chiral macromer of trimesic acid***

The macromers were characterized by variable angle attenuated total reflectance Fourier transform infrared (ATR-IR) spectroscopy to elucidate chemical structure of the chiral selective

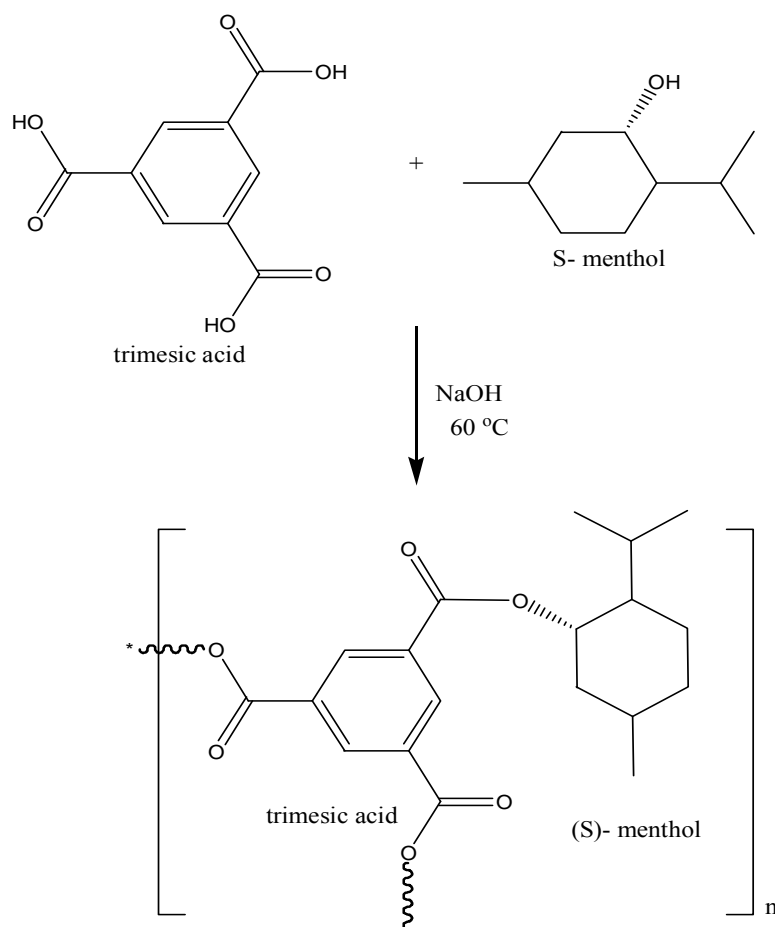


Fig. 1 Schematic representation of synthesis of macromer of S(-) menthol with trimesic acid

Table 2 Contact angle measurements of macromer and PI membrane

S. No.	Membrane code	Contact angle (radian)		
		Advancing	Receding	Mean
1	PI (Polyimide)	64.6	65.2	64.9
2	M1	70.8	70.4	70.6
3	M2	79.0	78.1	78.55

layer. This technique allows identification of main functional groups present on the surface of polyimide membrane thereby it is possible to establish the chemistry of the selective layer. ATR-FTIR spectra were recorded on Perkin-Elmer spectrometer (Perkin-Elmer, GX-1). The morphology of macromer was studied by scanning electron microscope (LEO, FESEM model 1430) using dried, fractured in dry ice and gold sputtered samples at a potential of 5-20 kV. The contact angle measurements of macromer given in Table 2 indicate an increase in hydrophilic nature of after the formation of co-polyester on the PI surface. The porosity analysis was done on

Table 3 Porosity analysis of macromer and PI membrane

S. No.	Membrane Code	Bubble point pressure (psi)	Bubble Point Pore Dia. ( $\mu$ )	Pore Dia. at Max. Pore Size Distribution
1	PI	34.064	0.3609	0.2056
2	M1	65.257	0.3534	0.1468
2	M2	71.357	0.1948	0.0960

Capillary Flow Porometer (Porous Materials Inc., USA, model 1500 AEX) using Porewick 'pore filling solution' having contact angle zero. The details of porosity analysis are given elsewhere (Singh and Bhattacharya 2006) (See Table 3).

### 2.2.3 Resolution of racemic menthol and ( $\pm$ ) *trans*-sobrerol

The optical resolution of aqueous solutions of racemic menthol and ( $\pm$ ) *trans*-sobrerol were performed in cross flow closed loop mode on reverse osmosis testing module. The testing module has four test cells connected in series. Each cell has a circular shape membrane of effective membrane area 0.00195 m<sup>2</sup>. Volumetric flux of aqueous solutions of racemic menthol and ( $\pm$ ) *trans*-sobrerol recorded at trans-membrane pressure 150 and 200 psi up to 40 h.

### 2.2.4 Analysis of permeates

The concentrations of menthol and ( $\pm$ ) *trans*-sobrerol enantiomers in permeates were determined by gas chromatography (GC 14B, Shimadzu) using chiral GC column (Beta-DEX 325), having pressure 1.2 bar was used for enantiomer excess determination. The compound for the analysis was first extracted in hexane and then analysed using GC.

## 2.3 Explanation

The performance of any membrane process is primarily judged by two most important parameters namely permeability and selectivity.

### 2.3.1 Permeability

The permeability describes how easily a fluid can flow through the porous material. The permeability of membranes is expressed as liquid permeability as well as solute permeability. The liquid permeability is the volume of liquid permeated through per unit area of membrane per unit time termed as volumetric flux ( $J_V$ ). The solute permeability is amount of solute passes through per unit area of membrane per unit time and is known as the solute flux ( $J_S$ ) which is calculated using volumetric flux and solute concentration in permeate according to following equation

$$J_S = Q / A_t \quad (1)$$

Here,  $Q$  is amount of solute permeated,  $A$  is area of membrane and  $t$  is permeation time.

### 2.3.2 Selectivity

The selectivity of membrane is expressed in terms of percentage rejection (%  $R$ ) given by following equation

$$\%R = (C_f - C_p / C_f) \times 100 \quad (2)$$

Here,  $C_p$  and  $C_f$  are concentrations of solute in permeate and feed respectively.

### 2.3.3 Enantioselectivity

The enantioselectivity of membrane is an important parameter to determine the performance of optical resolution process which defines the excess of one enantiomer over other enantiomer in permeate of membrane and is expressed as percentage enantiomeric excess (%ee) by following equation

$$\%ee = \frac{C^{Sp} - C^{Rp}}{C^{Sp} + C^{Rp}} \times 100 \quad (3)$$

Here,  $C^{Sp}$  and  $C^{Rp}$  are concentrations of S and R enantiomers in permeate.

Separation factor ( $\alpha$ ) is another important parameter to describe the enantiomeric separation. It is the ratios of enantiomers in permeate solution to feed solution as given by the following equation

$$\alpha = \frac{C^{Sp} / C^{Rp}}{C^{Sf} / C^{Rf}} \quad (4)$$

## 2.4 Characterization of macromer and PI membrane

The enantioselective macromer was characterized for pore size and surface morphology through microscopic observation. Microscopic observation is carried out by a scanning electron microscope (LEO, FESEM model 1430 VP, UK), which directly provides the visual information of the macromer morphology such as pore shape, size, their distribution and density. Computerized analysis of SEM image is a standard and widely used method for the investigation of perforated materials (Palacio *et al.* 1999, Kim and Fane 1994). For this study, SEM photographs are taken at different locations of the same membrane sheet from which the pore sizes are measured. This gives us the information regarding the number of pores in different pore size ranges from which percentage of pores in various pore size ranges.

The SEM photographs also provide us with the information regarding the structure and the presence of any micro voids in the sub layer of the membrane sheets. Some SEM photographs of chiral macromer and PI membrane are shown in Fig. 3. Some physical properties such as membrane thickness, pore diameter, and surface porosity of PI membrane are shown in Table 1.

## 2.5 Permeation experiment

The optical resolution of aqueous solutions of racemic menthol and ( $\pm$ )*trans*-sobrerol were performed in cross flow closed loop mode on reverse osmosis testing module. The testing module has four test cells connected in series. Each cell has a circular shape membrane of effective membrane area 0.00195 m<sup>2</sup>. Volumetric flux of aqueous solutions of racemic menthol and ( $\pm$ )*trans*-sobrerol recorded at trans-membrane pressure 150 and 200 psi up to 40 h. The sample solutions were collected from the permeate side after a permeation period and analyzed by GC using chiral column.

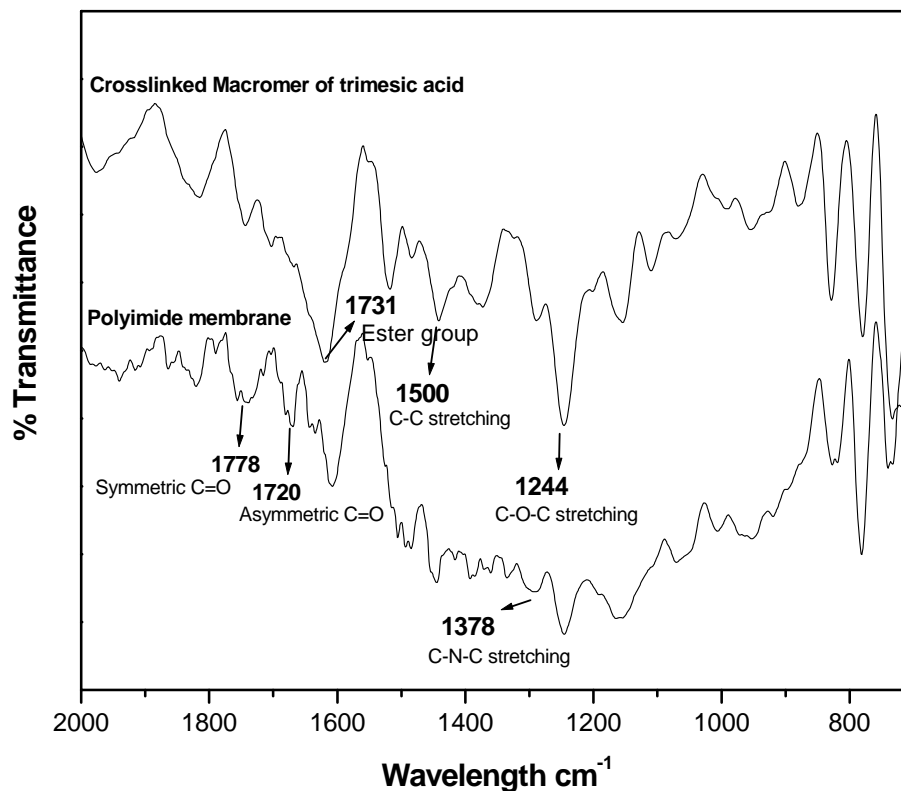


Fig. 2 ATR-FTIR spectra of polyimide (PI) and crosslinked macromer of trimesic acid

### 3. Results and discussions

#### 3.1 Characterization of the macromer and PI membrane

It is of interest to investigate the chemical composition of the membranes after esterification reaction. The ATR-FTIR spectrum of polyimide membrane exhibits a few characteristic bands as follows:  $1778\text{ cm}^{-1}$  (symmetric C=O stretching, imide),  $1722\text{ cm}^{-1}$  (asymmetric C=O stretching, imide), and  $1378\text{ cm}^{-1}$  (C–N–C stretching). The ATR-FTIR spectra of the macromer prepared by the polycondensation between trimesic acid and the hexane solution of *S*(-) menthol in Fig. 2 showed strong peaks at  $1731.15\text{ cm}^{-1}$ , which indicated the presence of the ester group. The peaks at  $1500\text{ cm}^{-1}$  and  $1245\text{ cm}^{-1}$  are from the C–C stretching of benzene ring and the C–O–C stretching of macromer prepared by the polycondensation respectively. This was formed by the reaction between –OH of menthol and –COOH of trimesic acid.

#### 3.2 Morphology of macromer and PI membrane

Fig. 3 shows the morphologies of the cross-sections and top surfaces of the macromer of trimesic acids as obtained from the FESEM analysis. Before the analysis, the material was snapped in liquid nitrogen to give a generally clean break for the cross-section scan. The resulting materials

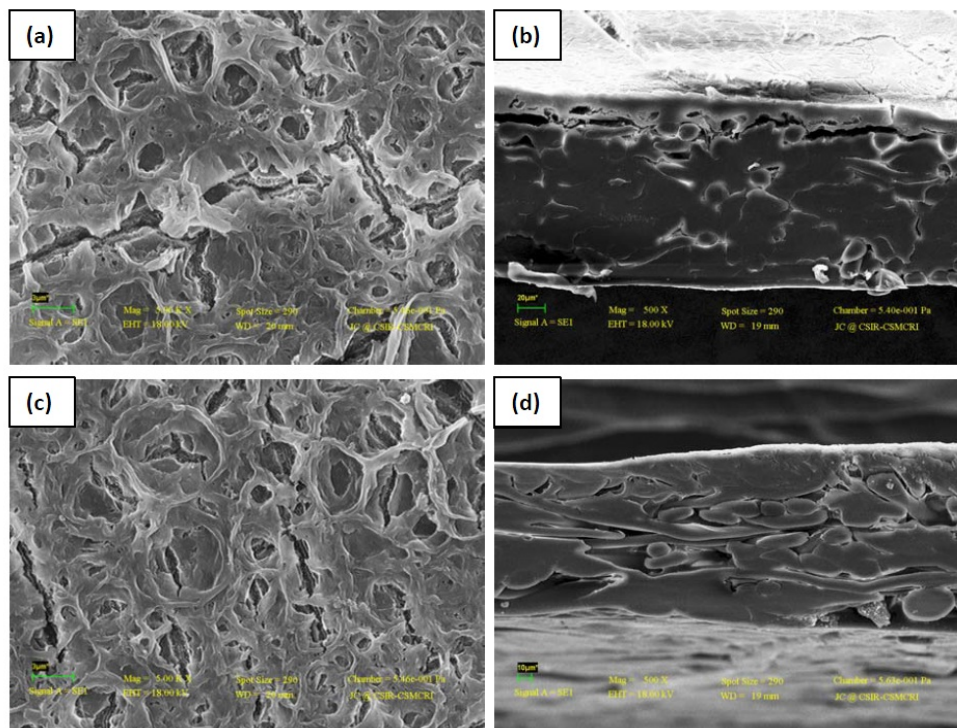


Fig. 3 Scanning electron micrographs of polyimide membrane and enantioselective chiral macromer layer: Polyimide membrane (a) surface and (b) cross-section, Enantioselective chiral macromer layer (c) surface and (d) cross-section

were coated with gold (Xiong *et al.* 2009). As can be seen by comparison with surface of both the membranes it's more or less similar but the cross-section of the PI membrane (Fig. 3b), and the macromer there is a clearly seen the difference in between them (Fig. 3d). It means there is macromere deposition on the surface of PI membrane.

All these supports the formation of co-polyester film on the polyimide support membrane. The surface morphology of materials as examined through scanning electron microscope of PI membrane (surface view and cross section) given in Figs. 3(a) and (b). In the Fig. 3d clearly shows three layers in the transverse view of crosslinked macromere that correspondence to non-woven polyester fabric, micro-porous polyimide layer and layer containing macromere deposition on the surface of PI membrane, the thickness of this macromer layer was approximately 0.5-1.0 micron.

Further, it could be seen that the film thicknesses increased with the increasing concentration of solutions. However, it is seen that there was little difference between the top surface of the PI membrane and the top surface of the chiral macromer layer because of macromere deposition on the surface of PI membrane (Figs. 3(a) and (c)).

### 3.3 Effect of monomer solutions concentration on polyimide membrane

The chiral macromer layer prepared using of 1-2% solution of trimesic acid in 60:40 water/MeOH, with 0.5-1% *S*(-) menthol (in hexane) at 60 °C obviously has more number of chiral

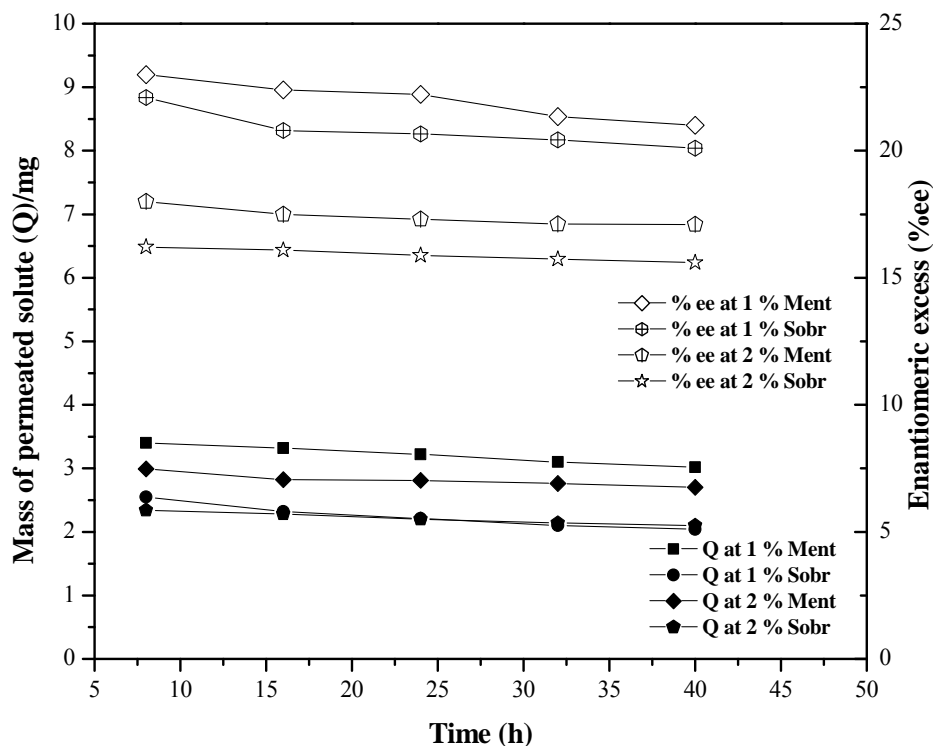


Fig. 4 Mass of permeated solute (Q) and % enantiomeric excess in the chiral separation of racemic menthol and ( $\pm$ ) *trans*-sobrerol through an enantioselective chiral macromer layer prepared with 1% and 2% *S*(-) menthol with trimesic acid. The feed concentration and operating pressure were 0.5 mg/mL and 150 psi, respectively

sites. As shown in Fig. 4 chiral macromer layer prepared from 1% menthol solution results high enantiomeric excesses compare with the macromer prepared from 2% menthol solution. The concentration of the feed solution has pronounced and adverse effect on %ee as seen in Fig. 4 because from concentrated feed too many solute molecules penetrate the macromer layer at a time however all molecules cannot interact to separation sites. The resolution through this material may take place as sorption-selective transport or diffusion-selective transport. The enantioselective macromer layer acts as barrier in resolution process and selectively transports one enantiomer due to stereo-specific interaction between enantiomer and chiral recognition sites present in the material. The transport of a solute through porous material could be explained either by pore flow model or by solution-diffusion model (Williams 2003).

As shown in Fig. 4 if the concentration of monomer solution for the formation of chiral macromer layer is increase the enantioselectivity is decreases due to thickness of chiral macromer layer. If used the more concentrated solution for the modification of chiral macromer layer the very thick layer is formed on the surface of polyimide membrane.

### 3.4 Effect of air-drying time of *S*(-) menthol solution on polyimide

The influence of the air-drying time of the *S*(-) menthol solution on the PI membrane when held in a vertical position from 10 min to over 20 min. With the increase in the air-drying time, the flux decreased and the %ee increased. Possible reasons may be that when the air-drying time was short, the PI substrate contained so much water and such a low concentration of *S*(-) menthol that only a small amount of macromer was produced by *S*(-) menthol and trimesic acid, resulting in low enantioselective selection and high flux. When the air-drying time extended beyond 20 min, the enantioselective chiral macromer layer was created by polycondensation on the surface of PI membrane, and over 23 %ee was obtained.

### 3.5 Effect of polycondensation time on the surface of PI membrane

The increase in time of polycondensation, the flux was reduced and the selectivity of enantioselective chiral macromer layer was increased. When this time was 3 min, over 23 %ee of enantioseparation was obtained. However, with the increase of the polycondensation time to 5 min, the flux was increased and the enantioselectivity of the chiral macromer significantly decreased, because we observed that the trimesic acid eroded PI, which resulted in the surface of the composite membrane being broken off. Therefore, the optimal time for interfacial polymerization was 3 min.

### 3.6 Effect of operating pressure

The mass of permeate solute and enantiomeric excess (%ee) of both the compounds in permeates as a function of permeation time at 150 psi and 200 psi pressures is given in Fig. 5. It is observed that higher enantiomeric excess is achieved at low permeation pressure. Fig. 5 shows the influence of the operating pressure on the enantiomeric separation of the racemic menthol and ( $\pm$ )*trans*-sobrerol. When the operating pressure increased from 150 psi to 200 psi, the flux increased and the %ee underwent a major reduction. The reason was that as the operating pressure increased, the diffusion of the racemic menthol and ( $\pm$ )*trans*-sobrerol were strengthened and the sorption to the racemic menthol and ( $\pm$ )*trans*-sobrerol were weakened, so the selectivity to the racemates was decreased and the flux was increased.

### 3.7 Effect of feed concentration of racemate

Fig. 6 shows the influence of the feed concentration on the chiral separation of racemic menthol and ( $\pm$ )*trans*-sobrerol racemates through the enantioselective chiral macromer layer. The flux increased significantly when the feed concentration was raised from 0.5 and 1.0 mg/mL; however, the enantiomeric excess decreased. This was probably because more and more active points became covered by the isomer, thus leading to the permeation of the other isomer. Another possible reason was that with the increase in feed concentration, the diffusion of the isomers interfered with each other. The enantioselectivity of chiral macromer layer was at its best when the feed concentration was 0.5 mg/mL.

Solute flux of racemic menthol and ( $\pm$ ) *trans*-sobrerol of concentrations 0.5% and 1.0% feed solution at 150 psi against permeation time was plotted (Fig. 6). The solute flux was observed to vaguely decrease up to 30 h, after which it stabilizes, may be due to united effect of solute rejection. The permeation of solute through chiral macromer layer is due to the combined effect of partition of solute in the material, preferential sorption and diffusion through the material

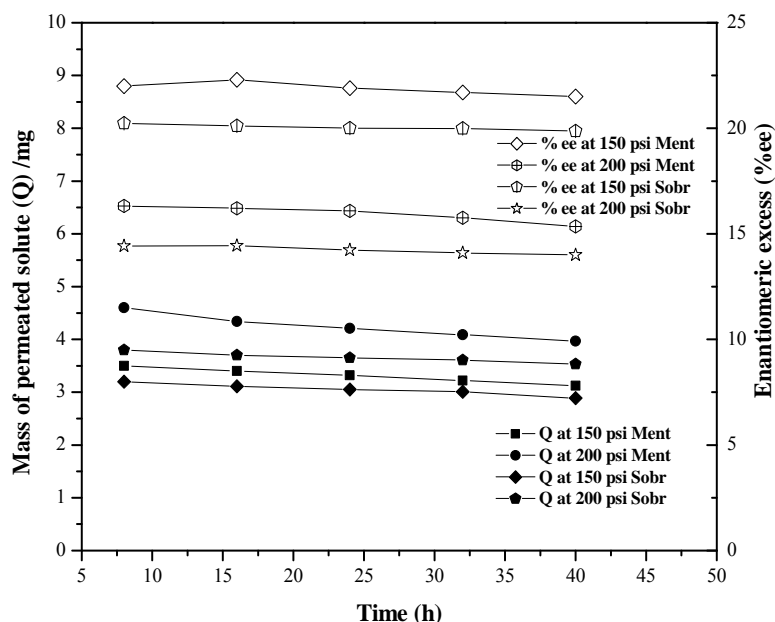


Fig. 5 Mass of permeated solute ( $Q$ ) and % enantiomeric excess in the chiral separation of racemic menthol and ( $\pm$ ) *trans*-sobrerol through enantioselective chiral macromer layer at 150 psi and 200 psi of operating pressure. The feed concentration was 0.5 mg/mL

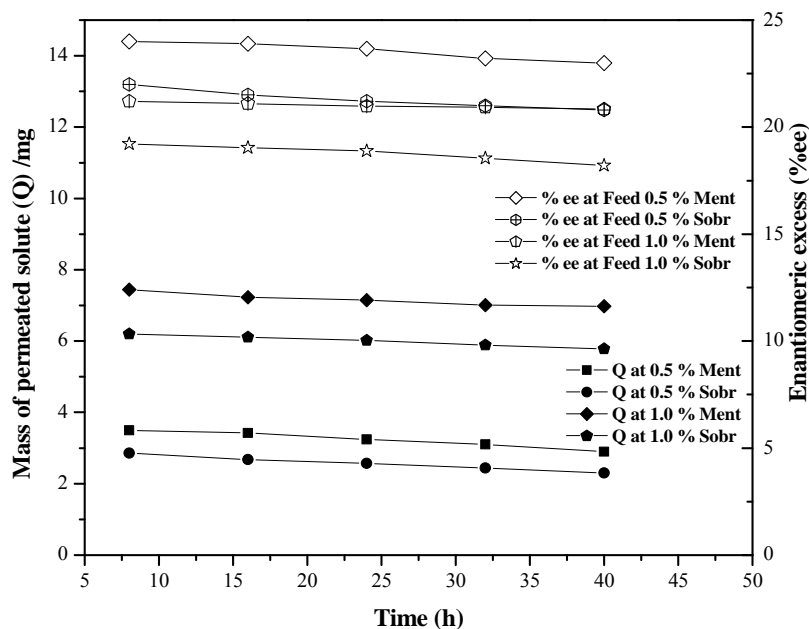


Fig. 6 Mass of permeated solute ( $Q$ ) and % enantiomeric excess in enantioseparation of racemic menthol and ( $\pm$ ) *trans*-sobrerol through enantioselective chiral macromer layer prepared with 1% *S*(-) menthol and 1% trimesic acid by polycondensation reaction. The feed concentrations were 0.5 mg/mL and 1.0 mg/mL respectively

(Kim and Jhon 1985, Twist and Zatz 2006, Manabu *et al.* 2005). The interaction between solute molecules and macromer surface mainly responsible for permeation of solute molecule are temporary and reversible therefore after certain period solute molecule get released into the flow stream leaving material interaction sites free.

#### 4. Conclusions

Chiral separation of racemic menthol and ( $\pm$ )*trans*-sobrerol were possible through a *S*(-) menthol crosslinked with trimesic acid chiral macromer layer using a pressure driven process. Chiral recognition was a result of the steric fit of the conformation of the enantiomers in the chiral space of the macromer, and of the molecular interactions between the racemate and the chiral macromer. The properties of the *S*(-) menthol crosslinked with trimesic acid chiral macromer layer were influenced by the air-drying time of the *S*(-) menthol solution on PI in a vertical position, the time of reaction, the operating pressure, and the feed concentration of the racemate.

#### Acknowledgments

Department of Science and Technology (DST), New Delhi-India and CSIR, New Delhi-India is gratefully acknowledged. We also wish to thanks Analytical Sciences Discipline of the institute for analytical support.

#### References

- Ahuja, S. (1991), *Chiral separation by liquid chromatography*, American Chemical Society, Washington.
- Aoki, T. (1999), "Macromolecular design of permselective membranes", *Prog. Polym. Sci.*, **24**(7), 951-993.
- Aoki, T., Kobayashi, Y., Kaneko, T., Oikawa, E., Yamamura, Y., Fujita, Y., Teraguchi, M., Nomura, R. and Masuda, T. (1999), "Synthesis and properties of polymers from disubstituted acetylenes with chiral pinanyl groups", *Macromolecules*, **32**(1), 79-85.
- Aoki, T., Ohshima, M., Shinohara, K., Kaneko, T. and Oikawa, E. (1997), "Enantioselective permeation of racemates through a solid (+)-poly{2-[dimethyl(10-pinanyl)silyl]norbornadiene} membrane", *Polymer*, **38**(1), 235-238.
- Aoki, T., Shinohara, K., Kaneko, T. and Oikawa, E. (1996), "Enantioselective permeation of various racemates through an optically-active poly(1-(dimethyl(10-pinanyl)silyl)-1-propyne) membrane", *Macromolecules*, **29**(12), 4192-4198.
- Aoki, T., Tomizawa, S. and Oikawa, E. (1995), "Enantioselective permeation through poly[ $\gamma$ -[3-(pentamethyldisiloxanyl)propyl]-L-glutamate] membranes", *J. Membrane. Sci.*, **99**(2), 117-125.
- Asztemborska, M., Sybilska, D., Nowakowski, R. and Perez, G. (2003), "Chiral recognition ability of  $\alpha$ -cyclodextrin with regard to some monoterpenoids under gas-liquid chromatographic conditions", *J. Chromatogr. A*, **1010**(2), 233-242.
- Baker, R.W. (2002), "Future directions of membrane gas separation technology", *Ind. Eng. Chem. Res.*, **41**(6), 1393-1411.
- Jacques, J. and Collet, A. (1981), *Enantiomers, racemates and resolutions*, Wiley Interscience, New York.
- Keurentjes, J.T.F., Nabuurs, L.J.W.M. and Vegter, E.A. (1996), "Liquid membrane technology for the separation of racemic mixtures", *J. Membrane. Sci.*, **113**(2), 351-360.

- Kim, K.J. and Fane, A.G. (1994), "Low voltage scanning electron microscopy in membrane research", *J. Membrane. Sci.*, **88**(1), 103-114.
- Kim, W.G. and Jhon, M.S. (1985), "The transport phenomena of some solute through the copolymer membranes of 2-hydroxyethylmethacrylate (HEMA) with selected hydrophobic monomers", *B. K. Chem. Soc.*, **6**, 128.
- Koros, W.J. and Fleming, G.K. (1993), "Membrane-based gas separation", *J. Membrane. Sci.*, **83**(1), 1-80.
- Koros, W.J. and Mahajan, R. (2000), "Pushing the limits on possibilities for large scale gas separation: which strategies?", *J. Membrane. Sci.*, **175**(2), 181-196.
- Lough, W.J. (1989), *Chiral liquid chromatography*, Chapman and Hall, New York.
- Lee, N.H. and Frank, C.W. (2002), "Separation of chiral molecules using polypeptide-modified poly(vinylidene fluoride) membranes", *Polymer*, **43**(23), 6255-6262.
- Lin, D.J., Chang, C.L., Chen, T.C. and Cheng, L.P. (2002), "Microporous PVDF membrane formation by immersion precipitation from water/TEP/PVDF system", *Desalination*, **145**(1-3), 25-29.
- Manabu, I., Hironobu, O. and Kiyoshi, M. (2005), "Specific permeation of hydrophobic solutes across a hydrophobic polymer membrane", *B. Chem. Soc. Jpn.*, **78**(9), 1702-1703.
- Maruyama, A., Adachi, N., Takatsuki, T., Torii, M., Sanui, K. and Ogata, N. (1990), "Enantioselective permeation of  $\alpha$ -amino acid isomers through poly(amino acid)-derived membranes", *Macromolecules*, **23**(10), 2748-2752.
- Nakamura, M., Kiyohara, S., Saito, K., Sugita, K. and Sugo, T. (1999), "High resolution of DL-tryptophan at high flow rates using a bovine serum albumin-multilayered porous hollow-fiber membrane", *Anal. Chem.*, **71**(7), 1323-1325.
- Newcomb, M., Helgeson, R.C. and Cram, D.J. (1974), "Enantiomer differentiation in transport through bulk liquid membranes", *J. Am. Chem. Soc.*, **96**(23), 7367-7369.
- Noble, R.D. (1992), "Generalized microscopic mechanism of facilitated transport in fixed site carrier membranes", *J. Membrane. Sci.*, **75**(1-2), 121-129.
- Nohira, H., Watanabe, K. and Kurokawa, M. (1976), "Optical resolution of N-benzyl-NNcis-2-aminocyclohexanecarboxylic acid by preferential crystallization", *Chem. Lett.*, **5**, 299-300.
- Palacio, L., Pradanos, P., Calvo, J.I. and Hernandez, A. (1999), "Porosity measurements by a gas penetration method and other techniques applied to membrane characterization", *Thin Solid Films*, **348**(1), 22-29.
- Ramdeehul, S., Dierkes, P., Aguado, R., Kamer, P.C.J., Van Leeuwen, P.W.N.M. and Osborn, J.A. (1998), "Mechanistic implications of the observation of kinetic resolution in a palladium-catalyzed enantioselective allylic alkylation", *Angew. Chem. Int. Ed.*, **37**(22), 3118-3121.
- Randon, J., Garnier, F., Rocca, J.L. and Maisterrena, B. (2000), "Optimization of the enantiomeric separation of tryptophan analogs by membrane processes", *J. Membrane. Sci.*, **175**(1), 111-117.
- Schurig, V. (2001), "Separation of enantiomers by gas chromatography", *J. Chromatogr. A*, **906**(1-2), 275-299.
- Shinohara, K., Aoki, T. and Oikawa, E. (1995), "Optical resolution by vapour permeation of 1,3-butanediol and 2-butanol through (+)-poly{1-[dimethyl(10-pinanyl)silyl]-1-propyne} membrane", *Polymer*, **36**(12), 2403-2405.
- Singh, K. and Bhattacharya, A. (2006), "Porometric study of Polysulfone membranes and their co-relation with the Performance", *J. Indian Chem. Soc.*, **83**, 201-204.
- Stern, S.A. (1994), "Polymers for gas separation: the next decade", *J. Membrane. Sci.*, **94**(1), 1-65.
- Stevenson, D. and Wilson, I.D. (1990), *Recent advances in chiral separation*, Plenum Press, New York.
- Teraguchi, M. and Masuda, T. (2002), "Poly(diphenylacetylene) membranes with high gas permeability and remarkable chiral memory", *Macromolecules*, **35**(4), 1149-1151.
- Teraguchi, M., Mottate, K., Kim, S.Y., Aoki, T., Kaneko, T., Hadano, S. and Masuda, T. (2005), "Synthesis of chiral helical poly(hydroxyl-containing phenylacetylene) membranes by in-situ depinanylsilylation and their enantioselective permeabilities", *Macromolecules*, **38**(15), 6367-6373.
- Teraguchi, M., Suzuki, J., Kaneko, T., Aoki, T. and Masuda, T. (2003), "Enantioselective permeation through membranes of chiral helical polymers prepared by depinanylsilylation of poly(diphenylacetylene) with a high content of the pinanylsilyl group", *Macromolecules*, **36**(26), 9694-9697.

- Twist, J.N. and Zatz, J.L. (1988), "Membrane-solvent-solute interaction in a model permeation system", *J. Pharmacol. Sci.*, **77**(6), 536-540.
- Ulbricht, M. (2006), "Advanced functional polymer membranes", *Polymer*, **47**(7), 2217-2262.
- Wang, D.L., Li, K. and Teo, W.K. (1999), "Preparation and characterization of polyvinylidene fluoride (PVDF) hollow fiber membranes", *J. Membrane. Sci.*, **163**(2), 211-220.
- Williams, M.E. (2003), *A review of reverse osmosis theory*, EET Corporation and Williams Engineering Services Company, Inc.
- Xiong, W.W., Wang, W.F., Zhao, L., Song, Q. and Yuan, L.M. (2009), "Chiral separation of (R,S)-2-phenyl-1-propanol through glutaraldehyde-crosslinked chitosan membranes", *J. Membrane. Sci.*, **328**(1-2), 268-272.
- Xu, H.W., Wang, Q.W., Zhu, J., Deng, J.G., Cun, L.F., Cui, X., Wu, J., Xu, X.L. and Wu, Y.L. (2005), "Copper(II)-mediated resolution of  $\alpha$ -halo carboxylic acids with chiral O,O'-dibenzoyltartaric acid: spontaneous racemization and crystallization-induced dynamic resolution", *Org. Biomol. Chem.*, **3**, 4227-4232.